Vacuum 89 (2013) 67–70

Contents lists available at SciVerse ScienceDirect

Vacuum

journal homepage: www.elsevier.com/locate/vacuum

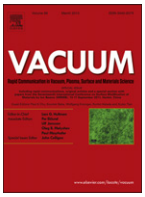

Rapid communication

Electroless deposition of Ni–W–P–B_4C nanocomposite coating on AZ91D magnesium alloy and investigation on its properties

A. Araghi*, M.H. Paydar

Department of Materials Science and Engineering, School of Engineering, Shiraz University, Zand Blvd., Shiraz, Iran

ARTICLE INFO

Article history:
Received 10 August 2012
Received in revised form
31 August 2012
Accepted 15 September 2012

Keywords:
Composite coating
Nanocrystalline
X-ray diffraction
Corrosion resistance

ABSTRACT

In the present work, electroless deposition of quaternary Ni–W–P–B_4C composite coatings on AZ91D magnesium alloy was investigated. The coatings were characterized to study their microstructure, crystallite size, morphology, microhardness and corrosion resistance and compared with Ni–P and Ni–P–B_4C composite coatings, prepared with the same method. The hardness of the Ni–W–P–B_4C composite coatings was around 1290 MPa which was more than that of the Ni–P and Ni–P–B_4C coatings (about 700 and 1200 MPa, respectively). According to polarization test results, the Ni–W–P–B_4C composite coating exhibits less and more corrosion rates with respect to the Ni–P–B_4C and the Ni–P coatings, respectively. X-ray diffraction (XRD) analysis results for the Ni–W–P–B_4C coating showed that the Ni–W–P–B_4C coating has a combination of amorphous and nanocrystalline structures. Also, Williamson–Hall analysis on the X-ray patterns revealed that the Ni–W–P–B_4C coating has an average crystallite size of 1.5 nm.

Magnesium and its alloys are used in various types of industrial applications such as aerospace, electronics and automotive, due to their high values of strength to weight ratio [1–4]. However, they have high reactivity, considerable corrosion rate in aqueous solutions, and poor wear resistance, which restrict their applications [2,3]. To improve magnesium alloys properties and overcome such drawbacks, coatings can be applied as a promising approach.

Ni–P coating is one of the most applied coatings to overcome the low corrosion resistance and high reactivity of magnesium alloys [1–3]. In the many researches the Ni–P coating can be applied simply by electroless deposition method, which not only require less apparatus but also would result in more uniform coatings with respect to other deposition methods such as electrodeposition, especially on substrates with a more complicated geometry [5–8]. In the present work, quaternary Ni–W–P–B_4C composite coatings was applied on AZ91D magnesium alloy by electroless method and its properties were compared with Ni–P and Ni–P–B_4C coatings, prepared with same method.

In this study, the substrates were chosen from AZ91D magnesium alloy and prepared to block shapes of 20 × 20 × 5 mm in dimension. In composite coatings, B_4C powders with an average size of 1.5–2 μm were used as reinforcement particles. To produce composite coatings, the definite amount of the B_4C particles (4 g/l) was added to the electroless plating bath. As mentioned before, AZ91D magnesium alloys are very active in aqueous solutions. Therefore, before the electroless deposition, the specimens were polished mechanically and then treated according to the CH + HFP pretreatment procedure. This pretreatment procedure includes three distinct steps in which the specimens are rinsed well by distilled water between them. More details of the pretreatment procedure are presented by other researchers [3].

In this research, to compare properties of Ni–W–P–B_4C coatings with Ni–P and Ni–P–B_4C coatings, the pretreated specimens were immersed in various types of electroless baths for 3 h to produce three different; Ni–W–P–B_4C, Ni–P–B_4C and Ni–P coatings. The chemical composition of the electroless bath for the Ni–W–P–B_4C coating was 15 g/l $NiSO_4 \cdot 6H_2O$, 14 g/l $NaH_2PO_2 \cdot H_2O$, 10 g/l Na_2WO_4, 13 g/l $NaC_2H_3O_2$, 12 ml/l HF(40% V/V), 8 g/l NH_4HF_2, 1 mg/l Thio urea, 4 g/l B_4C and for Ni–P coating was the same as the bath composition of Ni–W–P–B_4C without Na_2WO_4 and B_4C and for the Ni–P–B_4C coating was the same as the electroless bath composition of Ni–P where included 4 g/l B_4C particles. The pH and temperature for the bathes was 9 and 82 °C respectively. To maintain the B_4C particles suspended in the electroless bath, a magnetic stirrer device was used during the electroless deposition process.

A scanning electron microscope (SEM) Model Leo 440, 20 kV was used to evaluate the surface morphology of the coatings

---

* Corresponding author. Tel.: +98 917 416 1877; fax: +98 711 230 7293.
E-mail address: araghi.alirezaa@gmail.com (A. Araghi).

0042-207X/$ – see front matter © 2012 Elsevier Ltd. All rights reserved.
http://dx.doi.org/10.1016/j.vacuum.2012.09.011

(Fig. 1). As it can be seen, the Ni–W–P–B_4C coating has a nodular morphology and is uniformly well-compacted similar to Ni–P and Ni–P–B_4C coatings [9,10]. From Fig. 1, it can be also noted that the Ni–P coating is more compacted and homogenous as compared with the Ni–W–P–B_4C composite coating, while the distance between the peak to valley is lower in the Ni–W–P–B_4C composite coating as compared with Ni–P coating. This result can be due to the use of the magnetic stirrer during the electroless process of the composite coatings to avoid the B_4C particles sedimentation in the bath. Stirring and mixing the bath cause the compaction reduction and the uniformity increase of the coating [11].

Also, the phosphorus and tungsten content in the coatings was analyzed by a coupled EDX (Energy Dispersive X-ray analysis, Oxford) with SEM (Fig. 2). The EDX analysis of the coatings shows the Ni–P, Ni–P–B_4C and Ni–W–P–B_4C coatings contain 7.2, 6.5 and 5.1 %wt P respectively and the Ni–W–P–B_4C coating, 4.2 %wt W. Comparing the phosphorus peaks intensity in the compositional analysis by EDX shows that the addition of the B_4C particles to the composite coatings matrix has reduced the phosphorus content. In the same manner, a comparison of the Ni–P–B_4C and Ni–W–P–B_4C coating indicates a reduction in the phosphorus content when tungsten is added to the Ni–P–B_4C matrix. Tungsten atoms are dissolved substitutionaly in the FCC nickel matrix [6]. When tungsten atoms are located in the substitutional sites with larger atomic size ($r = 2.02$ Å) in comparison with nickel atom ($r = 1.62$ Å), the size of the sites that phosphorus atoms regularly occupied was reduced. Consequently, the solubility of phosphorus is reduced. In other words, in the coating with tungsten additives, less amount of phosphorus was observed [9].

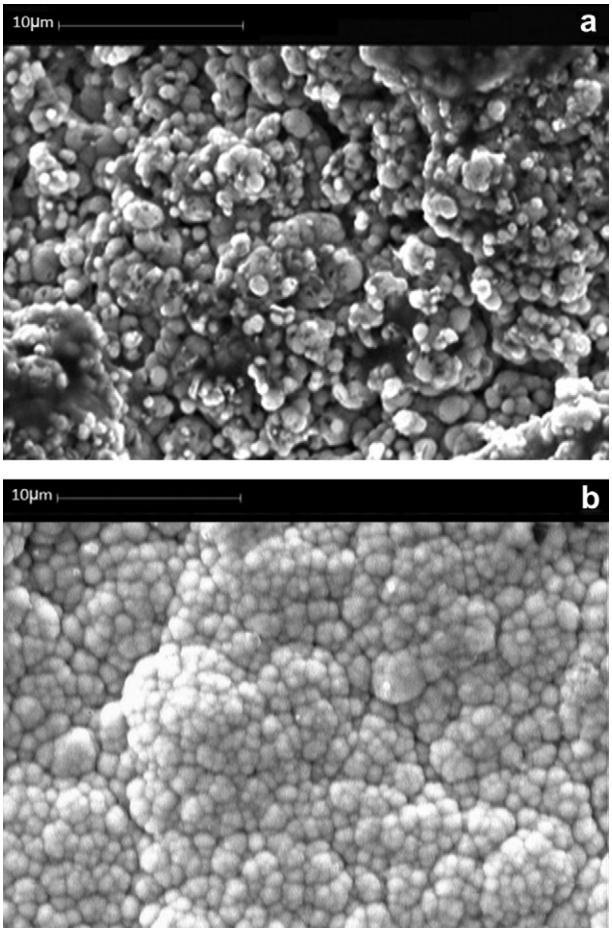

Fig. 1. SEM photographs of the electroless deposited: (a) Ni–W–P–B_4C composite and (b) Ni–P coatings, upon alloy AZ91D.

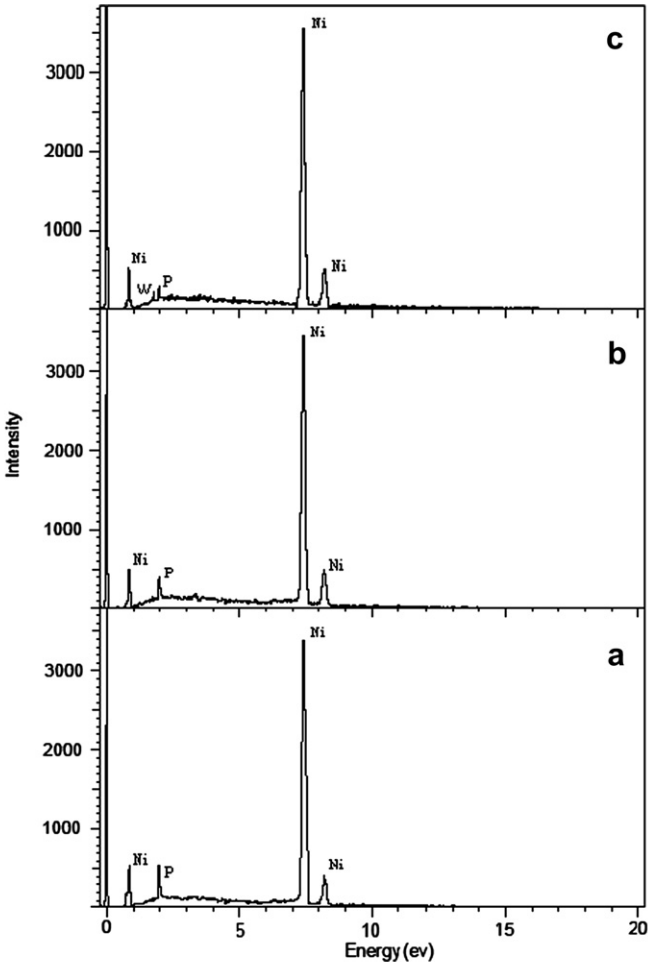

Fig. 2. EDX curves of (a) the Ni–P coating, (b) the Ni–P–B_4C coating and (c) the Ni–W–P–B_4C coating.

The crystallographic structure of the samples was studied via X-ray diffraction (XRD) with Philips X'pert diffractometer using Cu-Kα radiation with an angular step size of 0.05° at room temperature. The XRD analysis results for the Ni–W–P–B_4C, Ni–P–B_4C and Ni–P coatings are illustrated in Fig. 3. These graphs show that the Ni–W–P–B_4C and Ni–P–B_4C coatings have a combination of amorphous and nanocrystalline structures, the same as Ni–P coating [1–4]. The nickel crystallizes in the face centered cubic (FCC) system and the deposit is composed of small nickel FCC crystals supersaturated with phosphorus embedded in an amorphous Ni–P matrix. In other words phosphorus atoms in the nickel crystal lattice distort the lattice structure, disrupt the periodicity and produce an amorphous material.

In this study, Williamson–Hall analysis on the X-ray data were performed by calculating peak broadening in $2\theta = 44.7°$, $57.5°$ and $76.7°$. Table 1 illustrates the result of the Williamson–Hall analysis on the X-ray data, showing that the Ni–P, Ni–P–B_4C and Ni–W–P–B_4C coatings have the average grain size of 2.7, 1.9 and 1.5 nm, respectively. In addition, the values of lattice micro strain for the Ni–W–P–B_4C, Ni–P–B_4C and Ni–P coatings were determined to be -14×10^{-3}, -7×10^{-3} and $+6 \times 10^{-3}$, respectively. As it can be seen, tension lattice micro strain in the Ni–P coating changes to compression in the composite coatings. It could be related to the presence of the B_4C particles that creates compression strain in the